

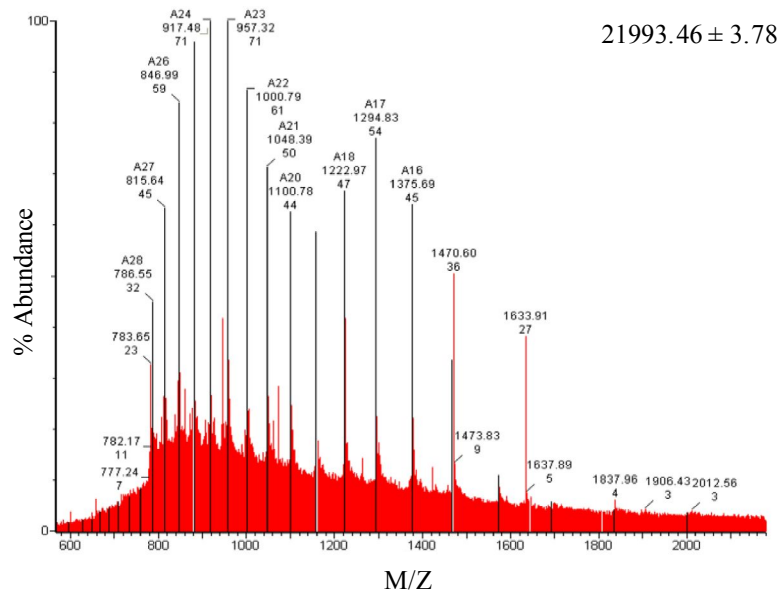
Supplementary Figure 1: Recombinant mouse GPIb α N and Mac-1 I-domain characterization. (a) Coomassie stained reducing SDS PAGE of purified recombinant mouse Mac-1 I-domain wild-type and Mac-1 I domain variant T209A, mouse GPIb α N wild type and variants GPIb α N E238A (E222 residue numbering without the signal sequence), GPIb α N H234A (H218 residue numbering without the signal sequence). (b) CD spectra of wild-type Mac-1 overlaid with spectra of the T209A and F302W mutants – all show practically identical spectra with the double minima at 208 and 222 nm characteristic of helix-rich structure; (c) corresponding CD spectrum of GPIb α N domain showing a strong negative ellipticity around 216 nm, consistent with the predominantly β -sheet structure (d) ¹H NMR spectrum of GPIb α N domain at 800 MHz showing excellent chemical shift dispersion and sharp resonances typical of a folded structure.

Query	Observed	Mr(expt)	Mr(calc)	ppm	Miss	Score	Expect	Rank	Unique	Peptide
4	1685.8926	1684.8853	1684.8744	6.45	1	81	1.1e-08	1	U	K.QGVDVKDTPNVA SVR.C
7	1815.8777	1814.8704	1814.8740	-1.97	0	23	0.018	1	U	R.HWLQENANNVYLWK.Q
9	2260.2163	2259.2090	2259.1634	20.2	0	167	3.3e-17	1	U	R.ELPSGLLDGLEDLDTLYLQR.N
10	2529.4133	2528.4061	2528.3486	22.7	1	106	2.7e-11	1	U	K.LRELPSGLLDGLEDLDTLYLQR.N

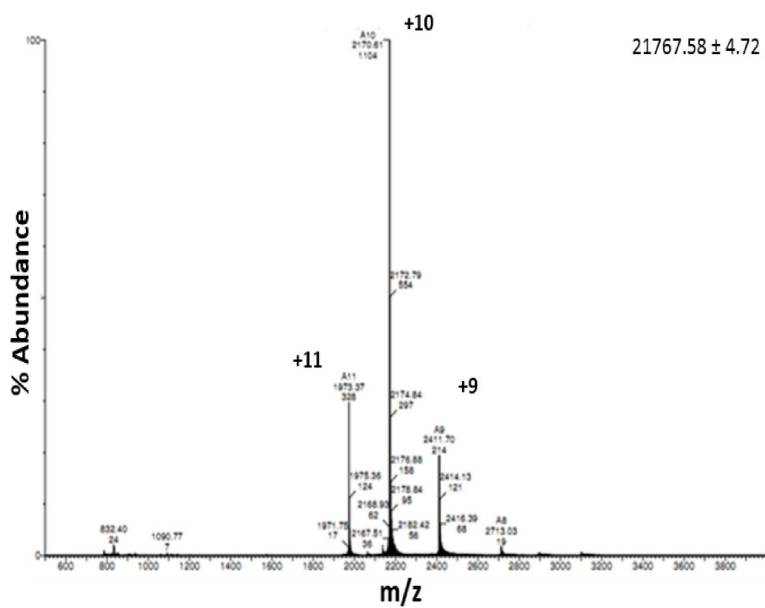
Query	Start – End	Observed	Mr(expt)	Mr(calc)	ppm	M	Score	Expect	Rank	U	Peptide
4	138 – 149	1236.6815	1235.6742	1235.7489	-60.4	0	83	1.3e-08	1	U	K.SLPPGLLLPTTK.L
10	160 – 181	2529.3203	2528.3130	2528.3486	-14.1	1	88	2.9e-09	1	U	K.LRELPSGLLDGLEDLDTLYLQR.N
9	162 – 181	2260.0317	2259.0245	2259.1634	-61.5	0	188	4.5e-19	1	U	R.ELPSGLLDGLEDLDTLYLQR.N
7	218 – 231	1756.8513	1755.8440	1755.8845	-23.0	0	72	1.4e-07	1	U	R.HWLQANANNVYLWK.Q
5	232 – 247	1685.7432	1684.7359	1684.8744	-82.2	1	122	1.7e-12	1	U	K.QGVDVKDTPNVA SVR.C
6	232 – 247	1685.8359	1684.8287	1684.8744	-27.2	1	92	1.7e-09	1	U	K.QGVDVKDTPNVA SVR.C
3	238 – 247	1059.4662	1058.4589	1058.5356	-72.5	0	44	8.3e-05	1	U	K.DTPNVA SVR.C

Query	Start – End	Observed	Mr(expt)	Mr(calc)	ppm	M	Score	Expect	Rank	U	Peptide
3	138 – 149	1236.7092	1235.7020	1235.7489	-38.0	0	78	3.6e-08	1	U	K.SLPPGLLLPTTK.L
9	162 – 181	2259.9702	2258.9629	2259.1634	-88.7	0	198	3.8e-20	1	U	R.ELPSGLLDGLEDLDTLYLQR.N
7	218 – 231	1748.8470	1747.8398	1747.8682	-16.2	0	100	2e-10	1	U	R.AWLQENANNVYLWK.Q
5	232 – 247	1685.7743	1684.7670	1684.8744	-63.8	1	112	1.7e-11	1	U	K.QGVDVKDTPNVA SVR.C

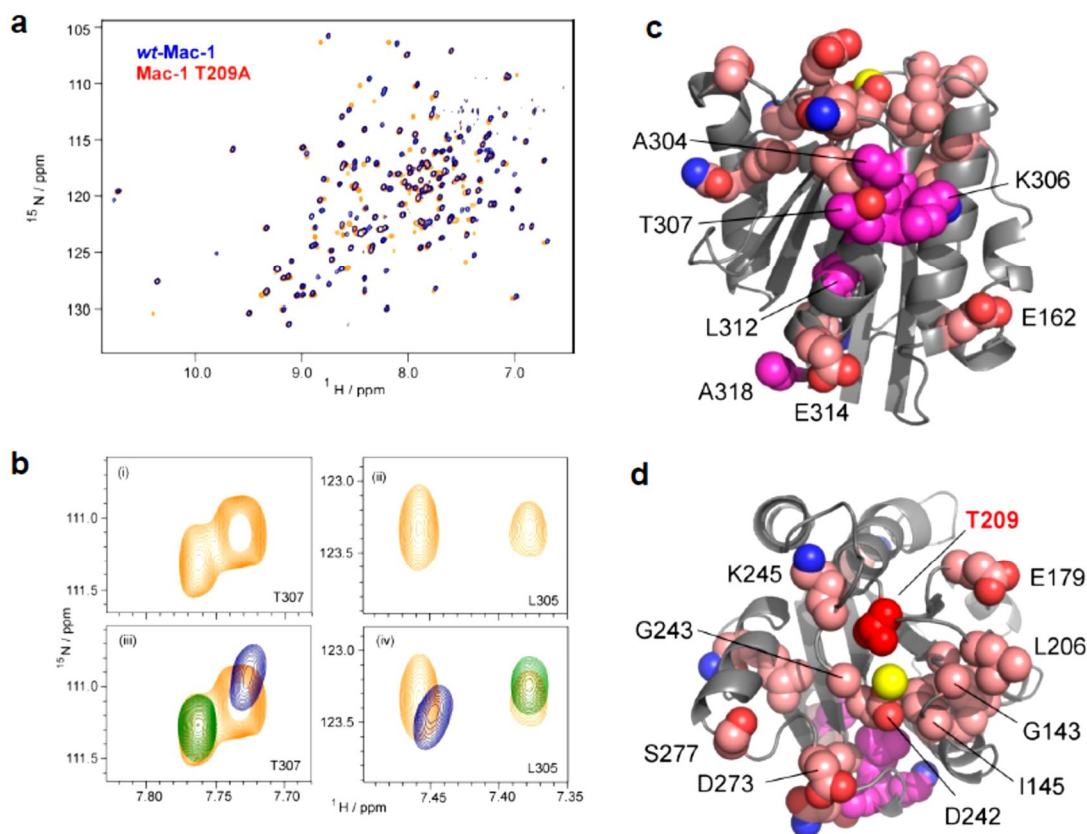
Supplementary Figure 2. Purified recombinant mouse GPIb α N domain characterisation. Summary of the fragments generated by the mass spectrometry of trypsin digested recombinant mouse GPIb α N wild type (top) and GPIb α N variants E238A (middle), H234A (bottom) confirming the sequence and mutation.



Supplementary Figure 3: Denatured ESI-MS spectrum of 10 μM ^{15}N -labeled mouse Mac-1 I-domain wild type in 1:1 water:acetonitrile with 1 % formic acid. The measured mass of 21993.46 ± 3.78 Da is in good agreement with the theoretical mass of 21996.6 Da.



Supplementary Figure 4: Native ESI-MS spectrum of 10 μM mouse Mac-1 T209A I-domain in 25 mM ammonium acetate. The measured mass of 21767.58 ± 4.72 Da is in good agreement with the theoretical mass of 21763.6 Da.



Supplementary Figure 5: NMR analysis of the Mac-1 T209A and F302W mutants. (a) overlaid HSQC spectra of wt-Mac-1 (blue) and T209A (orange); (b) cross-peaks from T307 (i) and L305 (ii) show peak doubling in the T209A spectrum (orange) and these are overlaid with spectra for wt-Mac-1 (blue) in (iii) and F302W (green) in (iv) showing similarities in peak positions; (c) CSP effects from the T209A mutation mapped to the structure of Mac-1 with the residues showing peak-doubling coloured pink, with other significantly perturbed peaks also highlighted; (d) top down view on to the MIDAS, showing T209 in red and surrounding residues perturbed by the mutation. The mutations show the significant structural plasticity of the I-domain which facilitates conformational changes distal to the point of mutation. Peak doubling in the T209A mutant shows that the protein is associated with multiple, dynamic conformational forms of similar energy which have features representative of the 'closed' and a 'pseudo-open' states in equilibrium. The T209A mutation demonstrates how perturbations to the co-ordination sphere around the MIDAS can be allosterically coupled to longer range conformational changes. The two conformations for the T209A mutant appear to be similar in energy (equally populated) in this context, showing the requisite structural plasticity to respond to ligand binding events.

Video 1: Video of the crystal structure of the mouse Mac-1 I-domain. A cartoon diagram is shown for the crystal structure of the mouse Mac-1 I-domain MIDAS face (purple) with the crystal contact stabilizing the active conformation derived from the C-terminal helix $\alpha 7$ in orange. The MIDAS bound Mg^{2+} ion is shown as a sphere (green) and key residues are shown as sticks and electrostatic interactions as dashed magenta lines (as shown in Figure 2b).

Video 2: Video of the Mac-1 I:GP1b α N complex interface. A cartoon diagram of the docked complex of the crystal structures of human GPIb α N and the Mac-1 I-domain interfacial region is shown. A close up view of the interface where the Mg^{2+} ion bound to the Mac-1 MIDAS site is shown as a sphere (green) and electrostatic interactions are shown as dashed purple lines. The GPIb α N C-terminal LRR capping region is colored orange and residue. GPIb α N residue D222 co-ordinates the Mac-1 MIDAS Mg^{2+} ion and surrounding residues on the MIDAS surface are colored light blue. F192 from the LRRs is in grey (as shown in Figure 4a).

Video 3: Video of the Mac-1 I:GP1b α N complex. A cartoon diagram of the docked complex of the crystal structures of human GPIb α N and the Mac-1 I-domain is shown. Secondary structures are colored blue/green and GPIb α N colored red/orange (as shown in Figure 4a).